9. New Developments in Laser Spectroscopy

During the last few years several new ideas have been born and new spectroscopic techniques have been developed that not only improve the spectral resolution and increase the sensitivity for investigating single atoms but that also allow several interesting experiments for testing fundamental concepts of physics. In the historical development of science, experimental progress in the accuracy of measurements has often brought about a refinement of theoretical models or even the introduction of new concepts [9.1]. Examples include A. Einstein's theory of special relativity based on the interferometric experiments of Michelson and Morley [9.2], M. Planck's introduction of quantum physics for the correct explanation of the measured spectral distribution of blackbody radiation, the introduction of the concept of electron spin after the spectroscopic discovery of the fine structure in atomic spectra [9.3], the test of quantum electrodynamics by precision measurements of the Lamb shift [9.4] or the still unresolved problem of a possible time dependence of physical fundamental constants, which might be solved by performing extremely accurate optical frequency measurements. In this chapter some of these new and exciting developments are presented.

9.1 Optical Cooling and Trapping of Atoms

In order to improve the accuracy of spectroscopic measurements of atomic energy levels, all perturbing effects leading to broadening or shifts of these levels must be either eliminated or should be sufficiently well understood to introduce appropriate corrections. One of the largest perturbing effects is the thermal motion of atoms. In Chap. 4 we saw that in collimated atomic beams the velocity components v_x and v_y, which are perpendicular to the beam axes, can be drastically reduced by collimating apertures (geometrical cooling). The component v_z can be compressed by adiabatic cooling into a small interval $v_z = u \pm \Delta v_z$ around the flow velocity u. If this reduction of the velocity distribution is described by a *translational temperature* T_{trans}, values of $T_{\text{trans}} < 1\,\text{K}$ can be reached. However, the molecules still have a nearly uniform but large velocity u, and broadening effects such as transit-time broadening or shifts caused by the second-order Doppler effect (see below) are not eliminated.

In this section we discuss the new technique of *optical cooling*, which decreases the velocity of atoms to a small interval around $v = 0$. Optical cooling down to "temperatures" of a few microKelvin has been achieved; by combining optical and evaporative cooling even the nanoKelvin range was reached.

This brought the discovery of quite new phenomena, such as Bose–Einstein condensation or atom–lasers, and atomic fountains. [9.5–9.7].

9.1.1 Photon Recoil

Let us consider an atom with rest mass M in the energy level E_i that moves with the velocity $\boldsymbol{v}$. If this atom absorbs a photon of energy $\hbar\omega_{ik} \simeq E_k - E_i$ and momentum $\hbar\boldsymbol{k}$, it is excited into the level E_k. Its momentum changes from $\boldsymbol{p}_i = M\boldsymbol{v}_i$ before the absorption to

$$\boldsymbol{p}_k = \boldsymbol{p}_i + \hbar\boldsymbol{k}\,, \tag{9.1}$$

after the absorption (the *recoil effect*, Fig. 9.1).

The relativistic energy conservation demands

$$\hbar\omega_{ik} = \sqrt{p_k^2c^2 + (M_0c^2 + E_k)^2} - \sqrt{p_i^2c^2 + (M_0c^2 + E_i)^2}\,. \tag{9.2}$$

When we extract $(M_0c^2 + E_k)$ from the first root and $(M_0c^2 + E_i)$ from the second, we obtain by a Taylor expansion the power series for the resonant absorption frequency

$$\omega_{ik} = \omega_0 + \boldsymbol{k}\cdot\boldsymbol{v}_i - \omega_0\frac{v_i^2}{2c^2} + \frac{\hbar\omega_0^2}{2Mc^2} + \ldots\,. \tag{9.3}$$

The first term represents the absorption frequency $\omega_0 = (E_k - E_i)$ of an atom at rest if the recoil of the absorbing atom is neglected. The second term describes the linear Doppler shift (first-order Doppler effect) caused by the motion of the atom at the time of absorption. The third term expresses the quadratic Doppler effect (second-order Doppler effect). Note that this term is independent of the direction of the velocity $\boldsymbol{v}$. It is therefore *not* eliminated by the "Doppler-free" techniques described in Chaps. 2–5, which only overcome the *linear* Doppler effect.

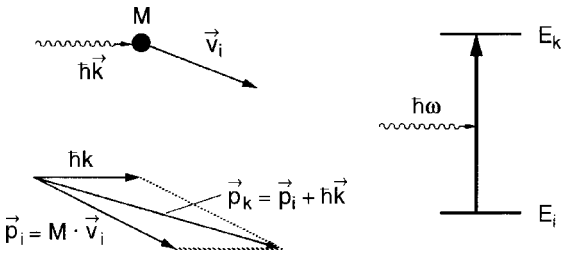

Fig. 9.1. Atomic recoil for absorption and emission of a photon

Example 9.1.
A parallel beam of Ne ions accelerated by 10 keV moves with the velocity $v_z = 3 \times 10^5$ m/s. When the beam is crossed perpendicularly by a single-mode laser beam tuned to a transition with $\lambda = 500$ nm, even ions with $v_x = v_y = 0$ show a quadratic relativistic Doppler shift of $\Delta\nu/\nu = 5 \times 10^{-7}$, which yields an absolute shift of $\Delta\nu = 250$ MHz. This should be compared with the linear Doppler shift of 600 GHz, which appears when the laser beam is parallel to the ion beam (Example 4.6).

The last term in (9.3) represents the recoil energy of the atom from momentum conservation. The energy $\hbar\omega$ of the absorbed photon has to be larger than that for recoil-free absorption by the amount

$$\Delta E = \frac{\hbar^2\omega_0^2}{2Mc^2} \quad \Rightarrow \quad \frac{\Delta E}{\hbar\omega} = \frac{1}{2}\frac{\hbar\omega}{Mc^2} \,. \tag{9.4}$$

When the excited atom in the state E_k with the momentum $\boldsymbol{p}_k = M\boldsymbol{v}_k$ emits a photon, its momentum changes to

$$\boldsymbol{p}_i = \boldsymbol{p}_k - \hbar\boldsymbol{k}$$

after the emission. The emission frequency becomes analogous to (9.3)

$$\omega_{ik} = \omega_0 + k\boldsymbol{v}_k - \frac{\omega_0 v_k^2}{2c^2} - \frac{\hbar\omega_0^2}{2Mc^2} \,. \tag{9.5}$$

The difference between the resonant absorption and emission frequencies is

$$\Delta\omega = \omega_{ik}^{\text{abs}} - \omega_{ki}^{\text{em}} = \frac{\hbar\omega_0^2}{Mc^2} + \frac{\omega_0}{2c^2}(v_k^2 - v_i^2) \approx \frac{\hbar\omega_0^2}{Mc^2} \,, \tag{9.6}$$

since the second term can be written as $(\omega_0/Mc^2)\cdot(E_k^{\text{kin}} - E_i^{\text{kin}})$ and $\Delta E^{\text{kin}} \ll \hbar\omega$. It can be therefore neglected for atoms with thermal velocities.

The relative frequency shift between absorbed and emitted photons because of recoil

$$\frac{\Delta\omega}{\omega} = \frac{\hbar\omega_0}{Mc^2} \,, \tag{9.7}$$

equals the ratio of photon energy to rest-mass energy of the atom.

For γ-quanta in the MeV range this ratio may be sufficiently large that $\Delta\omega$ becomes larger than the linewidth of the absorbing transition. This means that a γ-photon emitted from a free nucleus cannot be absorbed by another identical nucleus at rest. The recoil can be greatly reduced if the atoms are embedded in a rigid crystal structure below the Debye temperature. This recoil-free absorption and emission of γ-quanta is called the *Mössbauer effect* [9.8].

In the *optical region* the recoil shift $\Delta\omega$ is extremely small and well below the natural linewidth of most optical transitions. Nevertheless, it has been measured for selected narrow transitions [9.9, 9.10].

9.1.2 Measurement of Recoil Shift

When the absorbing molecules with the resonant absorption frequency ω_0 are placed inside the laser resonator, the standing laser wave of frequency $\omega \neq \omega_0$ burns two Bennet holes into the population distribution $N_i(v_z)$ (Fig. 9.2b and Sect. 2.2), which, according to (9.3), appear at the velocity components

$$v_{zi} = \pm[\omega' - \hbar\omega_0^2/(2Mc^2)]/k\,, \quad \text{with} \quad \omega' = \omega - \omega_0(1 - v^2/2c^2)\,. \tag{9.8}$$

The corresponding peaks in the population distribution $N_k(v_z)$ of molecules in the upper level $|k\rangle$ are shifted due to photon recoil (Fig. 9.2a). They show up, according to (9.5), at the velocity components

$$v_{zk} = \pm[\omega' + \hbar\omega_0^2/(2Mc^2)]/k\,. \tag{9.9}$$

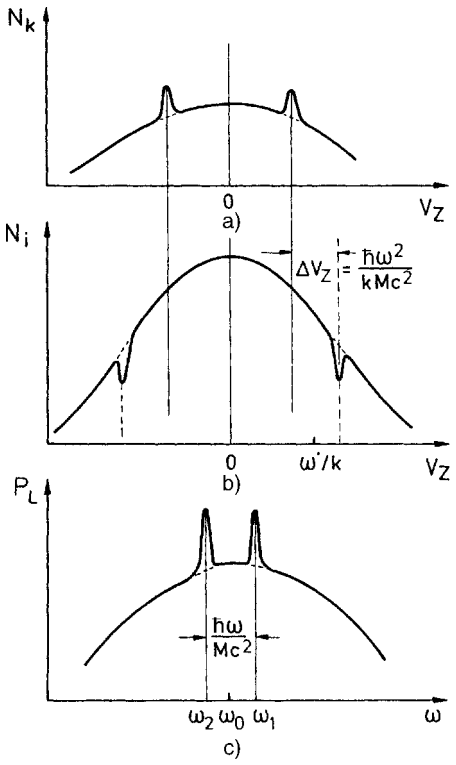

Fig. 9.2a–c. Generation of the recoil doublet of Lamb dips: (**a**) population peaks in the upper-state population for $\omega \neq \omega_0$; (**b**) Bennet holes in the lower-state population; (**c**)recoil doublet in the output power $P_L(\omega)$ of the laser

For the example, illustrated by Fig. 9.2, we have chosen

$$\omega < \omega_0 \;\Rightarrow\; \omega' < 0\,.$$

The two holes in the ground-state population coincide for $v_{zi} = 0$, which gives $\omega' = \hbar\omega_0^2/2Mc^2$. This happens, according to (9.8), for the laser frequency

$$\omega = \omega_1 = \omega_0[(1 - v^2/c^2) + \hbar\omega_0/(2Mc^2)]\,, \tag{9.10a}$$

while the two peaks in the upper level population coincide for another laser frequency

$$\omega = \omega_2 = \omega_0[(1 - v^2/c^2) - \hbar\omega_0/(2Mc^2)]\,. \tag{9.10b}$$

The absorption of the laser is proportional to the population difference $\Delta N = N_i - N_k$. This difference has two maxima at ω_1 and ω_2. The laser output therefore exhibits two Lamb peaks (*inverse Lamb dips*) (Fig. 9.2c) at the laser frequencies ω_1 and ω_2, which are separated by twice the recoil energy

$$\Delta\omega = \omega_1 - \omega_2 = \hbar\omega^2/Mc^2\,. \tag{9.11}$$

Example 9.2.

(a) For the transition at $\lambda = 3.39\,\mu\text{m}$ in the CH_4 molecule ($M = 16\,\text{AMU}$) the recoil splitting amounts to $\Delta\omega = 2\pi \cdot 2.16\,\text{kHz}$, which is still larger than the natural linewidth of this transition [9.10, 9.11].
(b) For the calcium intercombination line $^1S_0 \rightarrow {}^3P_1$ at $\lambda = 657\,\text{nm}$ we obtain with $M = 40\,\text{AMU}$ the splitting $\Delta\omega = 2\pi \cdot 23.1\,\text{kHz}$ [9.12].
(c) For a rotation–vibration transition in SF_6 at $\lambda = 10\,\mu\text{m}$ the frequency ω is one-third that of CH_4 but the mass 10 times larger than for CH_4. The recoil splitting therefore amounts only to about 0.02 kHz and is not measurable [9.14]

Since such small splittings can only be observed if the width of the Lamb peaks is smaller than the recoil shift, all possible broadening effects, such as pressure broadening and transit-time broadening, must be carefully minimized. This can be achieved in experiments at low pressures and with expanded laser beam diameters [9.13]. An experimental example is displayed in Fig. 9.3.

The velocities of very cold atoms are very small, i.e., the linear and the quadratic Doppler effects both become small and the recoil term becomes significant. It turns out that for cold Ca atoms at $T = 10\,\mu\text{K}$, the recoil effect leads to large asymmetries in the Lamb dips of absorption spectra taken with short pulses [9.15]. These are not found in experiments performed at room temperature, where the broad Doppler background masks these asymmetries, and they are based on the fundamental asymmetry between absorption and stimulated emission with short pulses.

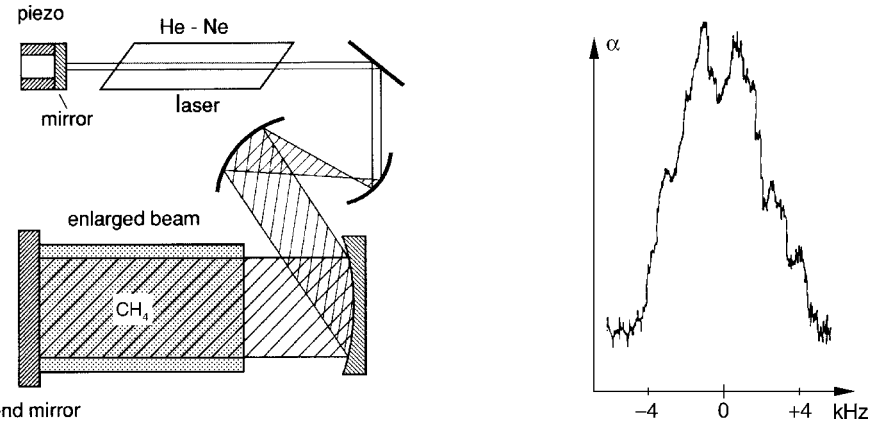

Fig. 9.3. Schematic experimental arrangement for measuring the recoil splitting and the measured signal of the recoil doublet of the hyperfine component $8 \rightarrow 7$ of the $(P(7), \nu_3)$ transition at $\lambda = 3.39\,\mu m$ in methane [9.11]

The transit-time broadening can greatly be reduced by the optical Ramsey method of separated fields. The best resolution of the recoil splittings has indeed been achieved with this technique (Sect. 9.4). The transit time can also be increased if only molecules with small transverse velocity components contribute to the Lamb dip. If the laser intensity is kept so small that saturation of the molecular transition is reached only for molecules that stay within the laser beam for a sufficiently long time, that is, molecules with small components v_x, v_y, the transit-time broadening is greatly reduced [9.11].

9.1.3 Optical Cooling by Photon Recoil

Although the recoil effect is very small when a single photon is absorbed, it can be used effectively for optical cooling of atoms by the cumulative effect of many absorbed photons. This can be seen as follows:

When atom A stays for the time T in a laser field that is in resonance with the transition $|i\rangle \rightarrow |k\rangle$, the atom may absorb and emit a photon $\hbar\omega$ many times, provided the optical pumping cycle is short compared to T and the atom behaves like a true two-level system. This means that the emission of fluorescence photons $\hbar\omega$ by the excited atom in level $|k\rangle$ brings the atom back only to the initial state $|i\rangle$, but never to other levels. With the saturation parameter $S = B_{ik}\rho(\omega_{ik})/A_{ik}$, the fraction of excited atoms becomes

$$\frac{N_k}{N} = \frac{S}{1+2S} .$$

The fluorescence rate is $N_k A_k = N_k/\tau_k$. Since N_k can never exceed the saturated value $N_k = (N_i + N_k)/2 = N/2$, the minimum recycling time for the saturation parameter $S \rightarrow \infty$ (Sect. 3.6) is $\Delta T = 2\tau_k$.

Example 9.3.

When an atom passes with a thermal velocity $v = 500\,\mathrm{m/s}$ through a laser beam with 2-mm diameter, the transit time is $T = 4\,\mu\mathrm{s}$. For a spontaneous lifetime $\tau_k = 10^{-8}\,\mathrm{s}$ the atom can undergo $q \leq (T/2)/\tau_k = 400$ absorption–emission cycles during its transit time.

When a laser beam is sent through a sample of absorbing atoms, the LIF is generally isotropic, that is, the spontaneously emitted photons are randomly distributed over all spatial directions. Although each emitted photon transfers the momentum $\hbar\boldsymbol{k}$ to the emitting atoms, the time-averaged momentum transfer tends to zero for sufficiently large values of $q = T/2\tau_k$.

The *absorbed* photons, however, all come from the same direction. Therefore, the momentum transfer for q absorptions adds up to a total recoil momentum $\boldsymbol{p} = q\hbar\boldsymbol{k}$ (Fig. 9.4). This changes the velocity $\boldsymbol{v}$ of an atom which flies against the beam propagation by the amount $\Delta v = \hbar k/M$ per absorption. For q absorption–emission cycles we get

$$\Delta v = q\frac{\hbar k}{M} = q\frac{\hbar\omega}{Mc}\,. \tag{9.12a}$$

Atoms in a collimated atomic beam can therefore be slowed down by a laser beam propagating anticollinearly to the atomic beam [9.16]. This can be expressed by the "cooling force"

$$\boldsymbol{F} = M\frac{\Delta\boldsymbol{v}}{\Delta T} = \frac{\hbar\boldsymbol{k}}{\tau_k}\frac{S}{1+2S}\,. \tag{9.12b}$$

Note that the *recoil energy* transferred to the atom

$$\Delta E_{\mathrm{recoil}} = q\frac{\hbar^2\omega^2}{2Mc^2}\,, \tag{9.13}$$

is still very small.

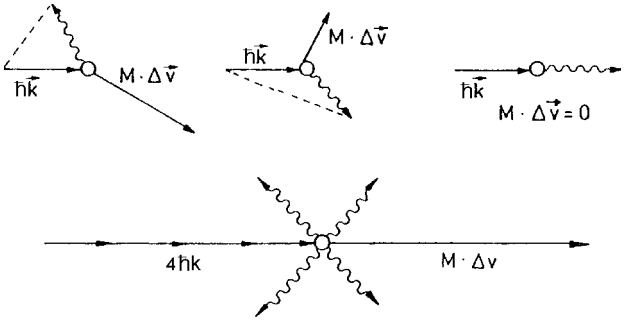

Fig. 9.4. Recoil momentum of an atom for a fixed direction of the absorbed photons but different directions of the emitted fluorescence photons

Example 9.4.

(a) For Na atoms with $M = 23$ AMU, which absorb photons $\hbar\omega \simeq 2$ eV on the transition $3\,^2S_{1/2} \rightarrow 3\,^2P_{3/2}$, (9.12) gives $\Delta v = 3$ cm/s per photon absorption. In order to reduce the initial thermal velocity of $v = 600$ m/s at $T = 500$ K to 20 m/s (this would correspond to a temperature $T = 0.6$ K for a thermal distribution with $\overline{v} = 20$ m/s),this demands $q = 2 \times 10^4$ absorption–emission cycles. At the spontaneous lifetime $\tau_k = 16$ ns a minimum cooling time of $T = 2 \times 10^4 \cdot 2 \cdot 16 \times 10^{-9}$ s $\simeq 600\,\mu$s is required. This gives a negative acceleration of $a = -10^6$ m/s^2, which is 10^5 times the gravity acceleration on earth $g = 9.81$ m/s^2! During the time T the atom has traveled the distance $\Delta_z = v_0 T - \frac{1}{2} a T^2 \simeq 18$ cm. During this deceleration path length it always has to remain within the laser beam. The total energy transferred by recoil to the atom is only -2×10^{-2} eV. It corresponds to the kinetic energy $\frac{1}{2} M v^2$ of the atom and is very small compared to $\hbar\omega = 2$ eV.

(b) For Mg atoms with $M = 24$ AMU, which absorb on the singlet resonance transition at $\lambda = 285.2$ nm, the situation is more favorable because of the higher photon energy $\hbar\omega \simeq 3.7$ eV and the shorter lifetime $\tau_k = 2$ ns of the upper level. One obtains: $\Delta v = -6$ cm/s per absorbed photon; $q = 1.3 \times 10^4$. The minimum cooling time becomes $T = 3 \times 10^{-5}$ s and the deceleration path length $\Delta z \simeq 1$ cm.

(c) In [9.17] a list of other atoms can be found that were regarded as possible candidates for optical cooling. Some of them have since been successfully tried.

The following remarks may be useful:

(a) Without additional tricks, this optical-cooling method is restricted to true two-level systems. Therefore, *molecules cannot be cooled with this technique*, because after their excitation into level $|k\rangle$ they return by emission of fluorescence into many lower vibrational–rotational levels and only a small fraction goes back into the initial level $|i\rangle$. Thus, only one optical pumping cycle is possible. There have been, however, other cooling mechanisms for molecules proposed and partly realized (see Sect. 9.1.5).

(b) The sodium transition $3S - 3P$, which represents the standard example for optical cooling, is in fact a multi level system because of its hyperfine structure (Fig. 9.5). However, after optical pumping with circularly polarized light on the hfs transition $3\,^2S_{1/2}(F'' = 2) \rightarrow 3\,^2P_{3/2}(F' = 3)$, the fluorescence can only reach the initial lower level $F'' = 2$. A true two-level system would be realized if any overlap of the pump transition with other hfs components could be avoided (see below).

(c) Increasing the intensity of the pump laser decreases the time ΔT for an absorption–emission cycle. However, for saturation parameters $S > 1$ this decrease is small and ΔT soon reaches its limit $2\tau_k$. On the other hand, the induced emission increases at the expense of spontaneous emission.

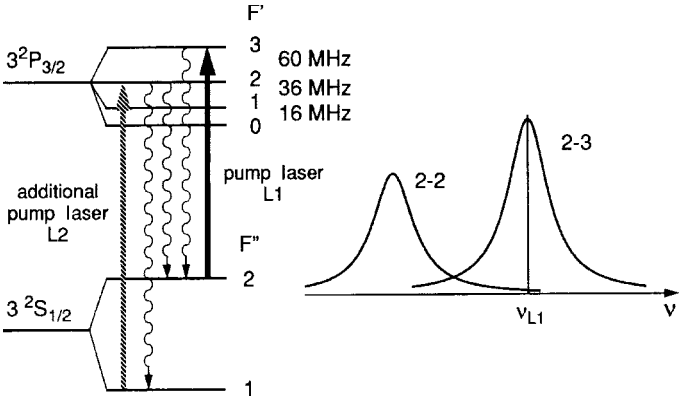

Fig. 9.5. Level diagram of the Na $3\,^2S_{1/2} \rightarrow 3\,^2P_{3/2}$ transition with hyperfine splittings. Optical pumping on the hfs component $F'' = 2 \rightarrow F' = 3$ represents a true two-level system, provided any overlap between the hfs components can be avoided. The additional pump laser L2 is necessary in order to pump atoms tranferred into level $F'' = 1$ by spectral overlap between the components $2 \rightarrow 3$ and $2 \rightarrow 2$ back into level $F'' = 2$

Since the emitted induced photon has the same $\boldsymbol{k}$-vector as the absorbed induced photon, the net momentum transfer is zero. The total deceleration rate therefore has a maximum at the optimum saturation parameter $S \simeq 1$.

9.1.4 Experimental Arrangements

For the experimental realization of optical cooling, which uses a collimated beam of atoms and a counterpropagating cw laser (dye laser or diode laser, Fig. 9.6) the following difficulties have to be overcome: during the decelera-

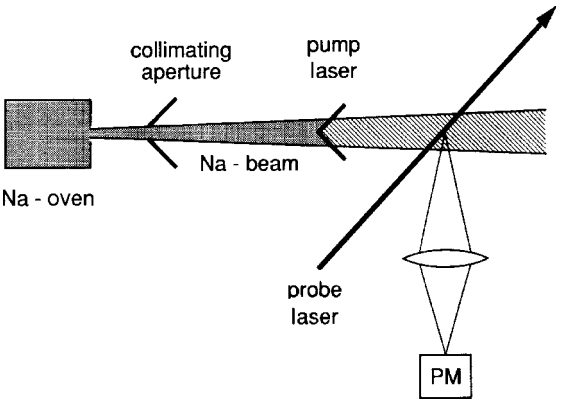

Fig. 9.6. Simplified experimental realization for the deceleration of atoms in a collimated beam by photon recoil

tion time the Doppler-shifted absorption frequency $\omega(t) = \omega_0 + \boldsymbol{k} \cdot \boldsymbol{v}(t)$ changes with the decreasing velocity v, and the atoms would come out of resonance with the monochromatic laser. Three solutions have been successfully tried: either the laser frequency

$$\omega(t) = \omega_0 + k \cdot v(t) \pm \gamma \,, \tag{9.14}$$

is synchronously tuned with the changing velocity $v(t)$ in order to stay within the linewidth γ of the atomic transition [9.18, 9.19], or the absorption frequency of the atom is appropriately altered along the deceleration path [9.20, 9.21]. A third alternative uses a broadband laser for cooling. We will discuss these methods briefly:

When the laser frequency ω for a counterpropagating beam $\boldsymbol{k}$ antiparallel to $\boldsymbol{v}$ is kept in resonance with the constant atomic frequency ω_0, it must have the time dependence

$$\omega(t) = \omega_0 \left(1 - \frac{v(t)}{c}\right) \quad \Rightarrow \quad \frac{\mathrm{d}\omega}{\mathrm{d}t} = -\frac{\omega_0}{c}\frac{\mathrm{d}v}{\mathrm{d}t} \,. \tag{9.15}$$

The velocity change per second for the optimum deceleration with a pump cycle period $T = 2\tau$ is, according to (9.12)

$$\frac{\mathrm{d}v}{\mathrm{d}t} = \frac{\hbar\omega_0}{2Mc\tau} \,. \tag{9.16}$$

Inserting this into (9.15) yields for the necessary time dependence of the laser frequency

$$\omega_\mathrm{L}(t) = \omega(0)(1 + \alpha t) \,, \quad \text{with} \quad \alpha = \frac{\hbar\omega_0}{2Mc^2\tau} \ll 1 \,. \tag{9.17}$$

This means that the pump laser should have a linear frequency chirp.

Example 9.5.

For Na atoms with $v(0) = 1000\,\mathrm{m/s}$, insertion of the relevant numbers into (9.17) yields $\mathrm{d}\omega/\mathrm{d}t = 2\pi \cdot 1.7\,\mathrm{GHz/ms}$, which means that fast frequency tuning in a controlled way is required in order to fulfill (9.17).

An experimental realization of the controlled frequency chirp uses amplitude modulation of the laser with the modulation frequency Ω_1. The sideband at $\omega_\mathrm{L} - \Omega_1$ is tuned to the atomic transition and can be matched to the time-dependent Doppler shift by changing $\Omega_1(t)$ in time. In order to compensate for optical pumping into other levels than $F'' = 2$ by overlap of the laser with other hfs components, the transition $F'' = 1 \rightarrow F' = 2$ is simultaneously pumped (Fig. 9.5). This can be achieved if the pump laser is additionally modulated at the second frequency Ω_2, where the sideband $\omega_\mathrm{L} + \Omega_2$ matches the transition $F'' = 1 \rightarrow F' = 2$ [9.19, 9.22].

For the second method, where the laser frequency ω_L is kept constant, the atomic absorption frequency must be altered during the deceleration of the atoms. This can be realized by Zeeman tuning (Fig. 9.7). In order to match the

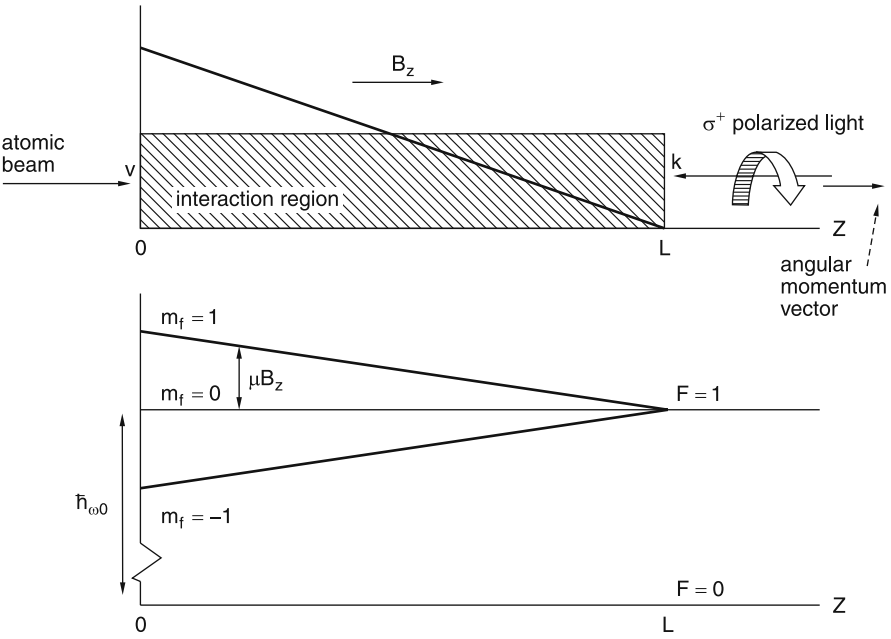

Fig. 9.7. Level diagram for laser cooling by Zeeman tuning

Zeeman shift to the changing Doppler shift $\Delta\omega(z)$, the longitudinal magnetic field must have the z-dependence

$$B = B_0\sqrt{1-2az/v_0^2}\,, \tag{9.18}$$

for atoms that enter the field at $z = 0$ with the velocity v_0 and experience the negative acceleration a [m/s^2] by photon recoil [9.21]. This field dependence $B(z)$ can be realized by a proper choice of the windings $N_W(z)$ per centimeters of the magnetic field coil (Fig. 9.8)

Most optical cooling experiments have been performed up to now on alkali atoms, such as Na or Rb, using a single-mode cw dye laser. The velocity decrease of the atoms is monitored with the tunable probe laser L2, which is sufficiently weak that it does not affect the velocity distribution. The probe-laser-induced fluorescence $I_{Fl}(\omega_2)$ is measured as a function of the Doppler shift. Experiments have shown that the atoms could be completely stopped and their velocity could even be reversed [9.18]. An example of the compression of the thermal velocity distribution into a narrow range around $v = 200\,\mathrm{m/s}$ is illustrated in Fig. 9.9 for Na atoms.

A favorable alternative to dye lasers is a GaAs diode laser, which can cool rubidium or cesium atoms [9.23–9.25] and also metastable noble gas atoms, such as He* or Ar* [9.26]. The experimental expenditures are greatly reduced since the GaAs laser is much less expensive than an argon laser plus dye-laser combination. Furthermore, the frequency modulation is more readily realized with a diode laser than with a dye laser.

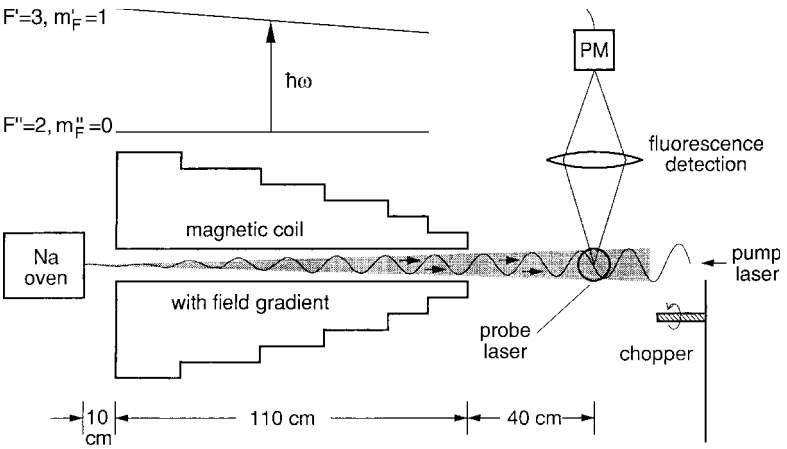

Fig. 9.8. Laser cooling of atoms in a collimated beam with a fixed laser frequency and Zeeman tuning of the atomic absorption frequency [9.21]

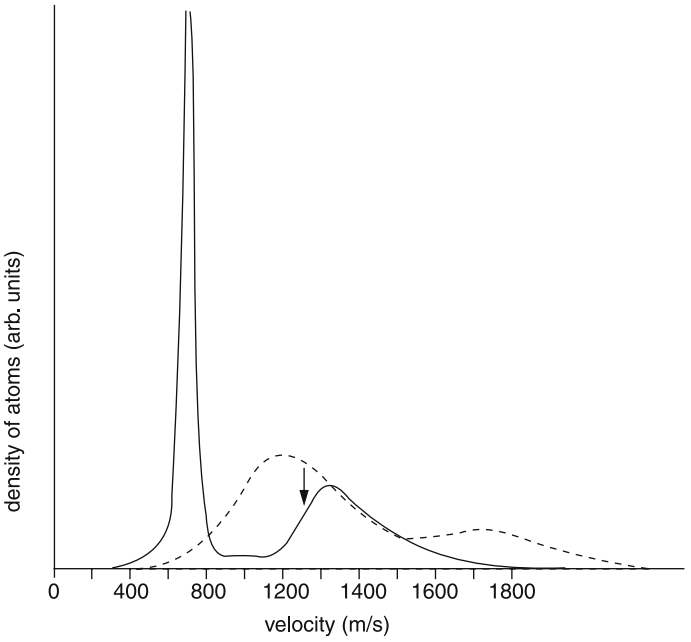

Fig. 9.9. Velocity distribution before (*dashed*) and after (*solid*) Zeeman cooling. The *arrow* indicates the highest velocity resonant with the slowing laser. (The extra bump at 1700 m/s is from $F = 1$ atoms, which are optically pumped into $F = 2$ during the cooling process) [W. Phillips, Nobel Lecture 1995]

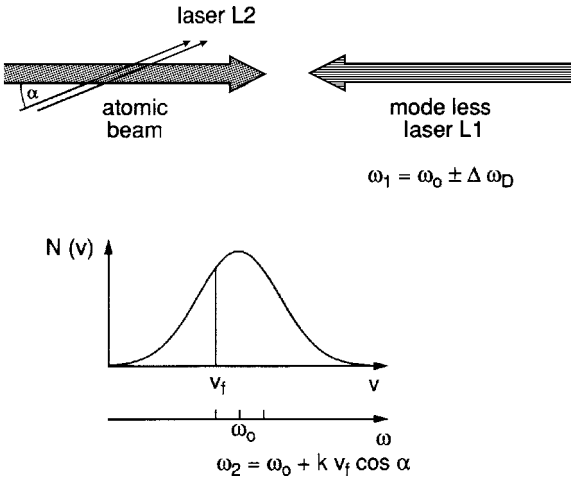

Fig. 9.10. Cooling of all atoms with a counterpropagating modeless laser. A cooling stop at a selectable velocity v_f can be realized with a second copropagating single-mode laser [9.29]

A very interesting alternative laser for optical cooling of atoms in a collimated beam is the *modeless* laser [9.27], which has a broad spectral emission (without mode structure, when averaged over a time of $T > 10$ ns, with an adjustable bandwidth and a tunable center frequency). Such a laser can cool all atoms regardless of their velocity if its spectral width $\Delta\omega_L$ is larger than the Doppler shift $\Delta\omega_D = v_0 k$ [9.28].

With the following experimental trick it is possible to compress the velocity distribution $N(v_z)$ of atoms in a beam into a small interval Δv_z around a wanted final velocity v_f. The beam from the modeless laser propagates anticollinearly to the atomic beam and cools the atoms (Fig. 9.10). A second single-mode laser intersects the atomic beam under a small angle α against the beam axis. If it is tuned to the frequency

$$\omega_2 = \omega_0 + k v_f \cos\alpha \,,$$

it accelerates the atoms as soon as they have reached the velocity v_f. This second laser therefore acts as a barrier for the lower velocity limit of cooled atoms [9.29].

The photon recoil can be used not only for the deceleration of collimated atomic beams but also for the deflection of the atoms, if the laser beam crosses the atomic beam perpendicularly [9.30–9.32]. In order to increase the transferred photon momentum, and with it the deflection angle, an experimental arrangement is chosen where the laser beam crosses the atomic beam many times in the same direction (Fig. 9.11). The deflection angle δ per absorbed photon, which is given by $\tan\delta = \hbar k/(m v_z)$, increases with decreasing atomic velocity v_z. Optically cooled atoms can therefore be deflected by large angles. Since the atomic absorption frequency differs for different isotopes, this

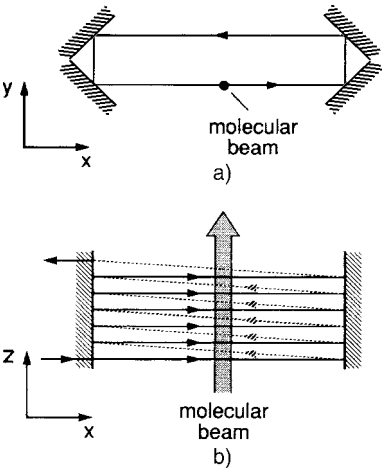

Fig. 9.11. Deflection of atoms in a collimated atomic beam using a multiple-path geometry. The molecular beam travels into the z-direction: (**a**) view into the z-direction; (**b**) view into the y-direction. On the *dashed* return paths the laser beam does not intersect the atomic beam

deflection can be used for spatial isotope separation [9.33] if other methods cannot be applied (Sect. 10.1.6).

An interesting application of atomic deflection by photon recoil is the collimation and focusing of atomic beams with lasers [9.34]. Assume atoms with the velocity $\boldsymbol{v} = \{v_x \ll v_z, 0, v_z\}$ pass through a laser resonator, where an intense standing optical wave in the $\pm x$-direction is present. If the laser frequency ω_L is kept slightly below the atomic resonance frequency ω_0 ($\gamma > \omega_0 - \omega_\mathrm{L} > 0$), atoms with transverse velocity components v_x are always pushed back to the z-axis by photon recoil because that part of the laser wave with the $\boldsymbol{k}$-vector antiparallel to v_x always has a larger absorption probabil-

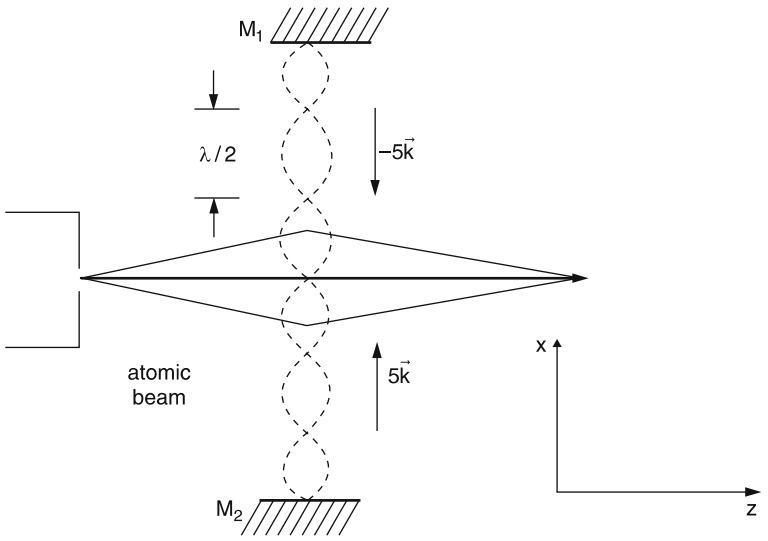

Fig. 9.12. Standing optical wave acting as a lens for a divergent atomic beam

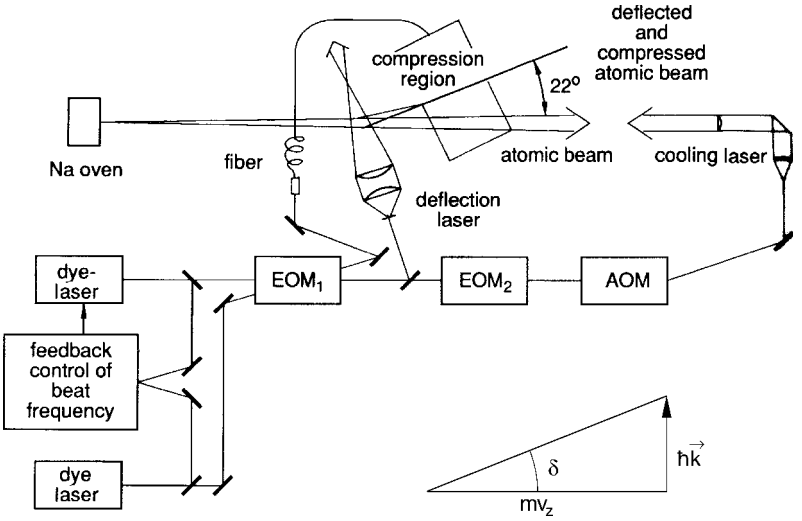

Fig. 9.13. Cooling, deflection and compression of atoms by photon recoil. The electro-optic modulators (EOM) and the acousto-optic modulator (AOM) serve for sideband generation and frequency tuning of the cooling laser sideband [9.32]

ity than the component with $\boldsymbol{k}$ parallel to v_x. The velocity component v_x is therefore reduced and the atomic beam is collimated.

If the atoms have been optically cooled before they pass the standing laser wave, they experience a large collimation in the maximum of the standing wave, but are not affected in the nodes. The laser wave acts like a transmission grating that "channels" the transmitted atoms and focuses the different channels (Fig. 9.12) [9.35].

A schematic diagram of an apparatus for optical cooling of atoms, deflection of the slowed-down atoms, and focusing is depicted in Fig. 9.13.

9.1.5 Threedimensional Cooling of Atoms; Optical Mollasses

Up to now we have only considered the cooling of atoms that all move into one direction. Therefore only one velocity component has been reduced by photon recoil. For cooling of atoms in a thermal gas where all three velocity components $\pm v_x$, $\pm v_y$, $\pm v_z$ have to be reduced, six laser beams propagating into the $\pm x$-, $\pm y$-, $\pm z$-directions are required [9.36]. All six beams are generated by splitting a single laser beam (Fig. 9.14). If the laser frequency is tuned to the red side of the atomic resonance ($\Delta\omega = \omega - \omega_0 < 0$), a repulsive force is always acting on the atoms, because for atoms moving toward the laser wave ($\boldsymbol{k} \cdot \boldsymbol{v} < 0$) the Doppler-shifted absorption frequency is shifted toward the resonance frequency ω_0, whereas for the counterpropagating wave ($\boldsymbol{k} \cdot \boldsymbol{v} > 0$) it is shifted away from resonance (Fig. 9.15). For a quantitative description we denote the absorption rate $R \propto \sigma(\omega)$ of an atom with $\boldsymbol{k} \cdot \boldsymbol{v} > 0$ by $R^+(v)$, and

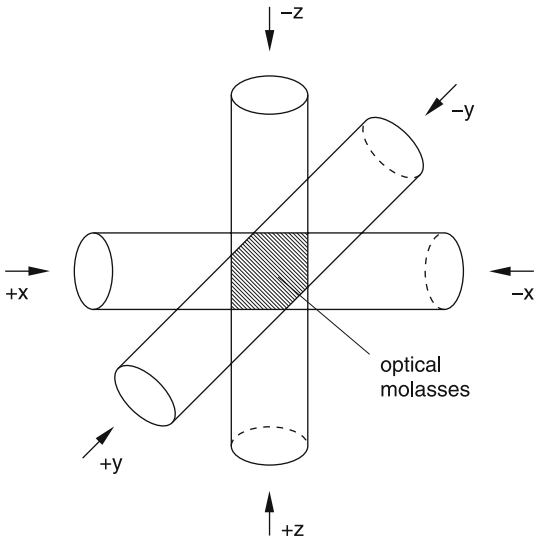

Fig. 9.14. Optical molasses with six pairwise counterpropagating laser beams

for $\boldsymbol{k}\cdot\boldsymbol{v}<0$ by $R^{-}(v)$. The net recoil force component F_i $(i=x,y,z)$ is then

$$F_i=[R^{+}(v_i)-R^{-}(v_i)]\cdot\hbar k\,. \tag{9.19}$$

For a Lorentzian absorption profile with FHWM γ, the frequency dependence of the absorption rate is (Fig. 9.15)

$$R^{\pm}(v)=\frac{R_0}{1+\left(\dfrac{\omega_{\mathrm{L}}-\omega_0\mp kv}{\gamma/2}\right)^2}\,. \tag{9.20}$$

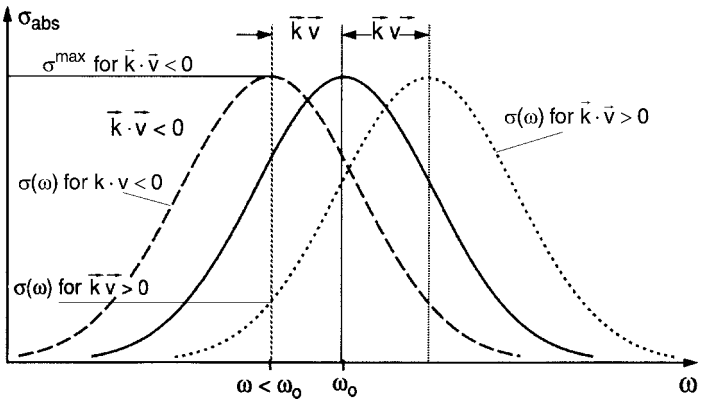

Fig. 9.15. For $\omega<\omega_0$, the absorption probability is larger for $\boldsymbol{k}\cdot\boldsymbol{v}<0$ than for $\boldsymbol{k}\cdot\boldsymbol{v}>0$

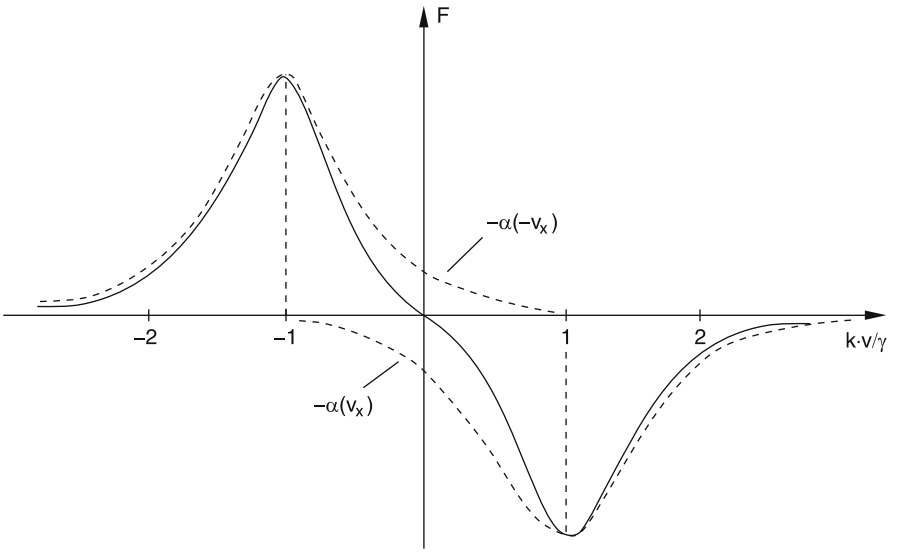

Fig. 9.16. Frictional force in an optical molasses (*solid curve*) for a red detuning $\delta = -\gamma$. The *dotted curve* shows the absorption profiles by a single atom moving with $v_x = \pm\gamma/k$ for a single laser beam propagating into the x-direction

Inserting (9.20) into (9.19) yields for $\boldsymbol{k}\cdot\boldsymbol{v} \ll \omega_{\mathrm{L}} - \omega_0 = \delta$ the net force (Fig. 9.16)

$$F_i = -a\cdot v_i\,, \quad \text{with} \quad a = R_0 \frac{16\delta\hbar k^2}{\gamma^2\left[1+(2\delta/\gamma)^2\right]^2}\,. \tag{9.21}$$

An atom moving within the overlap region of the six running laser waves therefore experiences a force $F_i(v_i) = -av_i$ $(i = x, y, z)$ that damps its velocity. From the relation $\mathrm{d}v/\mathrm{d}t = F/m \Rightarrow \mathrm{d}v/v = -a/m\,\mathrm{d}t$ we obtain the time-dependent velocity

$$v = v_0\,\mathrm{e}^{-(a/m)t}\,. \tag{9.22}$$

The velocity decreases exponentially with a damping time $t_{\mathrm{D}} = m/a$.

Example 9.6.

(a) For rubidium atoms ($m = 85$ AMU) the wavenumber is $k = 8\times10^6\,\mathrm{m}^{-1}$. At a detuning $\delta = \gamma$ and an absorption rate $R_0 = \gamma/2$ we obtain: $a = 4\times10^{-21}\,\mathrm{Ns/m}$. This gives a damping time $t = 35\,\mu\mathrm{s}$.

(b) For Na atoms with $\delta = 2\gamma$ one obtains $a = 1\times10^{-20}\,\mathrm{Ns/m}$ and $t_{\mathrm{D}} = 2.3\,\mu\mathrm{s}$. The atoms move in this light trap like particles in viscous molasses and therefore this atomic trapping arrangement is often called *optical molasses*.

Note: These optical trapping methods reduce the velocity components (v_x, v_y, v_z) to a small interval around $v = 0$. However, they do *not* compress the atoms into a spatial volume, except if the dispersion force for the field gradients $\nabla I \neq 0$ is sufficiently strong. This can be achieved by electric or magnetic field gradients, as discussed in Sect. 9.1.7.

9.1.6 Cooling of Molecules

The optical cooling techniques discussed so far are restricted to true two-level systems because the cooling cycle of induced absorption and spontaneous emission has to be performed many times before the atoms come to rest. In molecules the fluorescence from the upper excited level generally ends in many rotational–vibrational levels in the electronic ground state that differ from the initial level. Therefore most of the molecules cannot be excited again with the same laser. They are lost for further cooling cycles.

Cold molecules are very interesting for several scientific and technical applications. One example is chemical reactions initiated by collisions between cold molecules where the collision time is very long and the reaction probability might become larger by several orders of magnitude. In addition, interactions of cold molecules with surfaces where the sticking coefficient will be 100% open up new insights into molecule–surface interactions and reactions between cold adsorbed molecules. Finally, the possibility to reach Bose–Einstein condensation of molecular gases opens new fascinating aspects of collective molecular quantum phenomena.

There have been several proposals how molecules might be cooled in spite of the above-mentioned difficulties [9.37–9.39]. An optical version of these proposals is based on a frequency comb laser, which oscillates on many frequencies, matching the relevant frequencies of the transitions from the upper to the lower levels with the highest transition probabilities [9.39]. In this case, the molecules can be repumped into the upper level from many lower levels, thus allowing at least several pumping cycles.

A very interesting optical cooling technique starts with the selective excitation of a collision pair of cold atoms into a bound level in an upper electronic state (Fig. 9.17). While this excitation occurs at the outer turning point of the upper-state potential, a second laser dumps the excited molecule down into a low vibrational level of the electronic ground state by stimulated emission pumping (photo-induced association). In favorable cases the level $v = 0$ can be reached. If the colliding atoms are sufficiently cold, the angular momentum of their relative movement is zero (S-wave scattering). Therefore the final ground state has the rotational quantum number $J = 0$ if the two lasers transfer no angular momentum to the molecule (either two transitions with $\Delta J = 0$ or the absorbing and emission transition as R-transitions with $\Delta J = +1$ in absorption and -1 in emission) [9.40]. The kinetic energy of the molecule formed by photoassociation is always smaller than that of the colliding atoms because of momentum conservation [5.116].

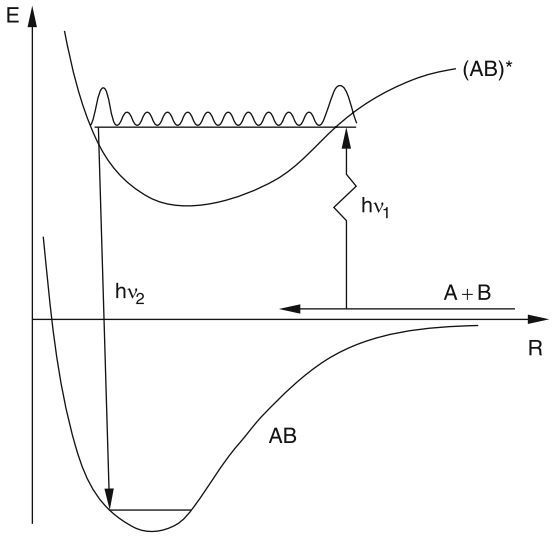

Fig. 9.17. Formation of cold molecules by photoassociation of a collision pair A+B

A promising nonoptical technique relies on cooling of molecules by collisions with cold atoms. If the gas mixture of atoms and molecules can be trapped in a sufficiently small volume long enough to achieve thermal equilibrium between atoms and molecules, the optically cooled atoms act as a heat sink for the molecules, which will approach the same temperature as the atoms (sympathetic cooling) [9.41].

An interesting proposal that could be realized uses a cold supersonic molecular beam with flow velocity u, which expands through a rotating nozzle (Fig. 9.18). We saw in Chap. 4 that in supersonic beams the velocity spread around the flow velocity u may become very small. The translational temperature in the frame moving with the velocity u can be as small as 0.1 K. If the nozzle moves with the speed $-v$, the molecules have the velocity $u - v$ in the laboratory frame. Tuning the angular velocity ω of the nozzle rotating on a circle with radius R makes it possible to reach any molecular velocity $v_m = u - \omega R$ between u and 0 in the laboratory frame. Since the beam must be collimated in order to reduce the other velocity components, there is only a small time interval per rotation period where the nozzle is in line with the collimating apertures. The cold molecules therefore appear as pulses behind the apertures.

An elegant technique has been developed in several laboratories, where cold helium clusters moving through a gas cell of atoms or molecules pick up these molecules, which then can diffuse into the interior of the helium cluster. The molecules then aquire the low temperature of the cluster. The binding energy is taken away by evaporation of He atoms from the cluster surface [9.42, 9.43].

At sufficiently low temperatures, the He droplet becomes superfluid [9.42]. The molecules inside the droplet can then freely rotate. Because the superfluid He droplet represents a quantum fluid with discrete excitation energies, the

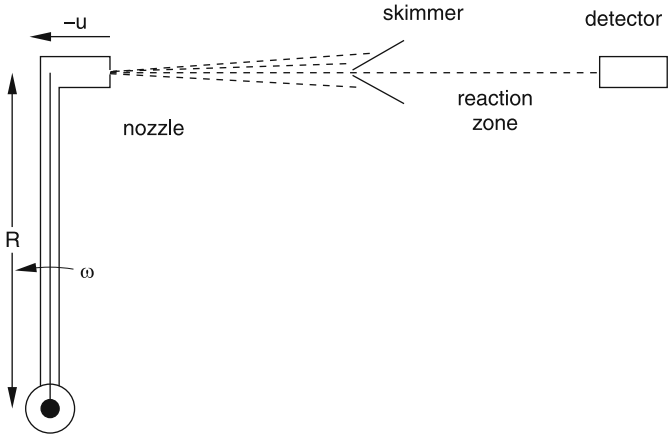

Fig. 9.18. Rotating nozzle for producing a beam of slow molecules

energy transfer between the molecule and its superfluid surroundings is limited and the molecular spectra show sharp lines. At the critical temperature between normal fluidity and superfluidity, the lines start to become broader. Laser spectroscopy of these molecules therefore gives direct information on the interaction of molecules and surroundings under different conditions from measured differences between the rotational spectrum of a free molecule and that for a molecule inside a cold He droplet. This has been verified for instance by M. Havenith and her group [9.42, 9.43].

Injecting different molecules into the He droplet gives the possibility to study chemical reactions between very cold molecules.

9.1.7 Optical Trapping of Atoms

The effectiveness of the optical molasses for cooling atoms anticipates that the atoms are trapped within the overlap region of the six laser beams for a sufficiently long time. This demands that the potential energy of the atoms shows a sufficiently deep minimum at the center of the trapping volume, that is, restoring forces must be present that will bring escaping atoms back to the center of the trapping volume.

We will briefly discuss the two most commonly used trapping arrangements. The first is based on induced electric dipole forces in inhomogeneous electric fields and the second on magnetic dipole forces in magnetic quadrupole fields. Letokhov proposed [9.46, 9.47] to use the potential minima of a three-dimensional standing optical field composed by the superposition of three perpendicular standing waves for spatial trapping of cooled atoms. It turns out that atoms can be indeed trapped this way, but only after they have been cooled down to very low temperatures. However, Ashkin and Gordon calculated [9.48] that the dispersion forces in focused Gaussian beams could be employed for trapping atoms.

a) Induced Dipole Forces in a Radiation Field

When an atom with the polarizability α is brought into an inhomogeneous electric field $\boldsymbol{E}$, a dipole moment $\boldsymbol{p} = \alpha \boldsymbol{E}$ is induced and the force

$$\boldsymbol{F} = -(\boldsymbol{p} \cdot \text{grad})\boldsymbol{E} = -\alpha(\boldsymbol{E} \cdot \nabla)\boldsymbol{E} = -\alpha[(\nabla \tfrac{1}{2}E^2) - \boldsymbol{E} \times (\nabla \times \boldsymbol{E})] \,, \quad (9.23)$$

acts onto the induced dipole. The same relation holds for an atom in an optical field. However, when averaging over a cycle of the optical oscillation the last term in (9.23) vanishes, and we obtain for the mean dipole force [9.49]

$$\langle \boldsymbol{F}_\mathrm{D} \rangle = -\frac{1}{2}\alpha \nabla (E^2) \,. \quad (9.24)$$

The polarizability $\alpha(\omega)$ depends on the frequency ω of the optical field. It is related to the refractive index $n(\omega)$ of a gas with the atomic density N (Sect. 3.1.3) by $\alpha \approx \epsilon_0(\epsilon - 1)/N$. With $(\epsilon - 1) = n^2 - 1 \approx 2(n-1)$ we obtain

$$\alpha(\omega) = \frac{2\epsilon_0[n(\omega) - 1]}{N} \,. \quad (9.25)$$

Inserting (3.37b) for $n(\omega)$, the polarizability $\alpha(\omega)$ becomes

$$\alpha(\omega) = \frac{e^2}{2m_\mathrm{e}\omega_0} \frac{\Delta\omega}{\Delta\omega^2 + (\gamma_\mathrm{s}/2)^2} \,, \quad (9.26)$$

where m_e is the electron mass, $\Delta\omega = \omega - (\omega_0 + \boldsymbol{k} \cdot \boldsymbol{v})$ is the detuning of the field frequency ω against the Doppler-shifted eigenfrequency $\omega_0 + \boldsymbol{kv}$ of the atom, and $\gamma_\mathrm{s} = \delta\omega_\mathrm{n}\sqrt{1+S}$ is the saturation-broadened linewidth characterized by the saturation parameter S (Sect. 3.6).

For $\Delta\omega \ll \gamma_\mathrm{s}$ the polarizability $\alpha(\omega)$ increases nearly linearly with the detuning $\Delta\omega$. From (9.24) and (9.26) it follows that in an intense laser beam ($S \gg 1$) with the intensity $I = \epsilon_0 c E^2$ the force $\boldsymbol{F}_\mathrm{D}$ on an induced atomic dipole is

$$\boldsymbol{F}_\mathrm{D} = -a\Delta\omega\nabla I \,, \quad \text{with} \quad a = \frac{e^2}{m\epsilon_0 c\gamma^2\omega_0 S} \,. \quad (9.27)$$

This reveals that in a homogeneous field (for example, an extended plane wave) $\nabla I = 0$ and the dipole force becomes zero. For a Gaussian beam with the beam waist w propagating in the z-direction, the intensity $I(r)$ in the x–y-plane is, according to (5.32)

$$I(r) = I_0 \, \mathrm{e}^{-2r^2/w^2} \,, \quad \text{with} \quad r^2 = x^2 + y^2 \,.$$

The intensity gradient $\nabla I = -(4r/w^2) I(r)\hat{\boldsymbol{r}}$ points into the radial direction and the dipole force $\boldsymbol{F}_\mathrm{D}$ is then directed toward the axis $r = 0$ for $\Delta\omega < 0$ and radially outwards for $\Delta\omega > 0$.

For $\Delta\omega < 0$ the z-axis of an intense Gaussian laser beam with $I(r=0) = T_0$ represents a minimum of the potential energy

$$E_{\text{pot}} = \int_0^\infty F_{\text{D}}\,\mathrm{d}r = +a\Delta\omega I_0\,, \tag{9.28}$$

where atoms with sufficiently low radial kinetic energy may be trapped. In the focus of a Gaussian beam we have an intensity gradient in the r-direction as well as in the z-direction. If the two forces are sufficiently strong, atoms can be trapped in the focal region.

Besides this dipole force in the r- and z-directions the recoil force in the $+z$-direction acts onto the atom (Fig. 9.19). In a standing wave in $\pm z$-direction the radial force and the recoil force may be sufficiently strong to trap atoms in all directions. For more details see [9.50–9.52].

Example 9.7.

In the focal plane of a Gaussian laser beam with $P_{\text{L}} = 200\,\text{mW}$ focused down to a beam waist of $w = 10\,\mu\text{m}$ ($I_0 = 1.2\times10^9\,\text{W/m}^2$), the radial intensity gradient is $\partial I/\partial r = 2r/w^2 I_0\,\mathrm{e}^{-2r^2/w^2}$, which gives for $r = w$: $(\partial I/\partial r)_{r=w} = 2I_0/w\cdot\mathrm{e}^2$. With the number above one obtains:$(\partial I/\partial r)_{r=w} = 2.4\times10^{13}\,\text{W/m}^3$ and the radial dipole force acting on a Na atom is for $\Delta\omega = -|\gamma| = -2\pi\cdot10^7\,\text{s}^{-1}$, $S = 0$, and $r = w$

$$\boldsymbol{F}_{\text{D}} = +a\Delta\omega\frac{4r}{w^2}I_0\hat{\boldsymbol{r}}_0 = 1.5\times10^{-16}\,\text{N}\,,$$

The axial intensity gradient is for a focusing lens with $f = 5\,\text{cm}$ and a beam diameter $\partial I/\partial z = 4.5\times10^5\,\text{W/m}^3$. This gives an axial dipole force of $F_{\text{D}}(z) = 3\times10^{-24}\,\text{N}$, while the recoil force is about

$$\boldsymbol{F}_{\text{recoil}} = 3.4\times10^{-20}\,\text{N}\,.$$

In the axial direction the recoil force is many orders of magnitude larger than the axial dipole force. The potential minimum with respect to the radial dipole force is $E_{\text{pot}} \simeq -5\times10^{-7}\,\text{eV}$. In order to trap atoms in this minimum their radial kinetic energy must be smaller than $5\times10^{-7}\,\text{eV}$, which corresponds to the "temperature" $T \simeq 5\times10^{-3}\,\text{K}$.

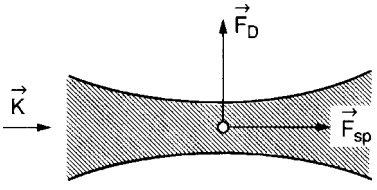

Fig. 9.19. Longitudinal and transverse forces on an atom in the focus of a Gaussian beam

Example 9.8.

Assume a standing laser wave with $\lambda = 600\,\text{nm}$, an average intensity $I = 10\,\text{W/cm}^2$, and a detuning of $\Delta\omega = \gamma = 60\,\text{MHz}$. The maximum force acting on an atom because of the intensity gradient $\nabla I = 6 \times 10^{11}\,\text{W/m}^3$ between maxima and nodes of the field becomes, according to (9.27), with a saturation parameter $S = 10$: $F_\text{D} = 10^{-17}\,\text{N}$. The trapping energy is then $1.5 \times 10^{-5}\,\text{eV} \hat{\approx} T = 0.15\,\text{K}$.

Example 9.8 demonstrates that the negative potential energy in the potential minima (the nodes of the standing wave for $\Delta\omega > 0$) is very small. The atoms must be cooled to temperatures below 1 K before they can be trapped.

Another method of trapping cooled atoms is based on the net recoil force in a three-dimensional light trap, which can be realized in the overlap region of six laser beams propagating into the six directions $\pm x$, $\pm y$, $\pm z$.

b) Magneto-Optical Trap

A very elegant experimental realization for cooling and trapping of atoms is the magneto-optical trap (MOT), which is based on a combination of optical molasses and an inhomogeneous magnetic quadrupole field (Fig. 9.21). Its principle can be understood as follows:

In a magnetic field the atomic energy levels E_i experience Zeeman shifts

$$\Delta E_i = -\boldsymbol{\mu}_i \cdot \boldsymbol{B} = -\mu_\text{B} \cdot g_F \cdot m_F \cdot B\,, \tag{9.29}$$

which depend on the Lande g-factor g_F, Bohr's magneton μ_B, the quantum number m_F of the projection of the total angular momentum F onto the field direction, and on the magnetic field B.

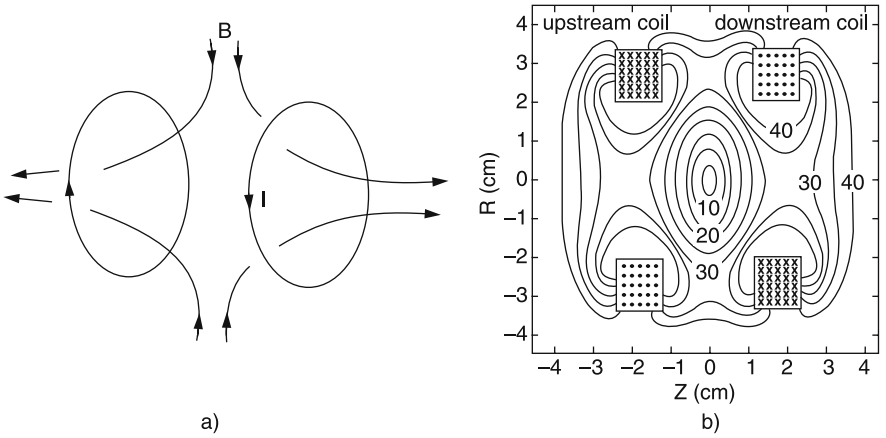

Fig. 9.20a,b. Magnetic field of the MOT: (**a**) magnetic field lines; (**b**) equipotential lines

In the MOT the inhomogeneous field is produced by two equal electric currents flowing into opposite directions through two coils with radius R and distance $D = R$ (anti-Helmholtz arrangement) (Fig. 9.20). If we choose the z-direction as the symmetry axis through the center of the coils, the magnetic field around $z = 0$ in the middle of the arrangement can be described by the linear dependence

$$B = bz \, . \tag{9.30}$$

where the constant b depends on the current through the coil and the size of the anti-Helmholtz coils. The Zeeman splittings of the transition from $F = 0$ to $F = 1$ are shown in Fig. 9.21b. Atoms in the center of this MOT are exposed to the six red-tuned laserbeams of the optical molasses (Fig. 9.21e). Let us at first only consider the two beams in the $\pm z$-direction, where the laserbeam in $+z$-direction is σ^+ polarized. Then the reflected beam in the $-z$ direction is σ^- polarized. For an atom at $z = 0$ where the magnetic field is zero, the absorption rates are equal for both laser beams, which means that the average momentum transferred to the atom is zero. For an atom at $z > 0$, however, the σ^--beam is preferentially absorbed because here the frequency

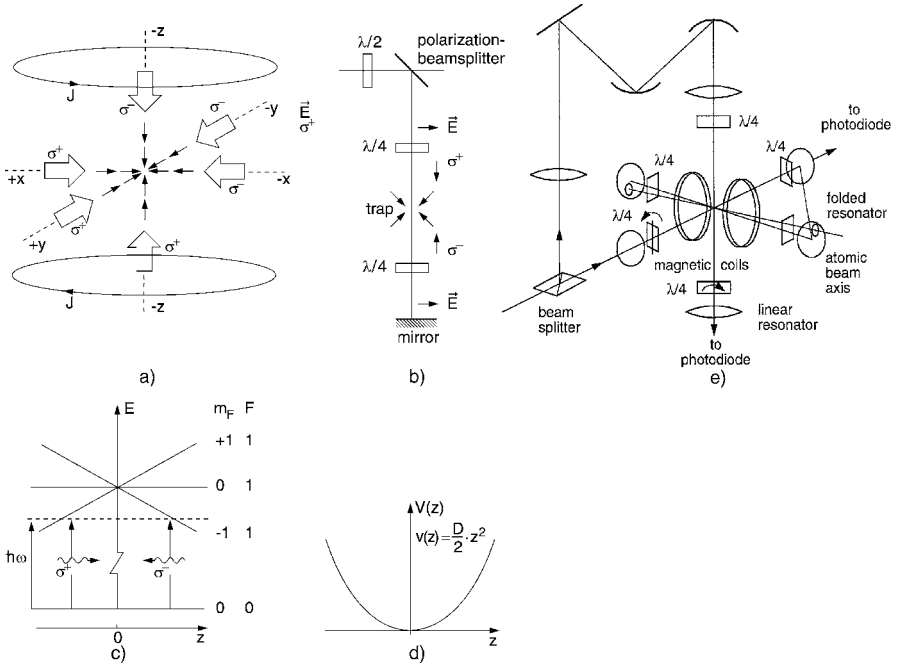

Fig. 9.21a–e. Magneto-optical trap. (**a**) Optical molasses inside the center of an inhomogeneous magnetic field; (**b**) preparation of one of the three laser beams; (**c**) level scheme illustrating the principle of the MOT; (**d**) potential of the MOT; (**e**) schematic experimental setup

difference $\omega_L - \omega_0$ is smaller than for the σ^+-beam. This means that the atom experiences a net momentum transfer into the $-z$-direction, back to the center.

In a similar way an atom at $z < 0$ shows a preferential absorption of σ^+-light and gets a net momentum in the $+z$-direction. This shows that the atoms in the MOT are compressed toward the trap center.

We will now discuss this spatially dependent restoring force more quantitatively.

From the above discussion the net force

$$\boldsymbol{F}(z) = R_{\sigma^+}(z)\hbar\boldsymbol{k}_{\sigma^+} + R_{\sigma^-}(z)\hbar\boldsymbol{k}_{\sigma^-} , \tag{9.31}$$

is determined by the difference of the absorption rates R_{σ^+}, R_{σ^-} (note that the wave vectors are antiparallel). For a Lorentzian absorption profile with halfwidth γ, the absorption rates become

$$R_{\sigma^\pm} = \frac{R_0}{1 + \left[\dfrac{\omega_L - \omega_0 \pm \mu b z/\hbar}{\gamma/2}\right]} . \tag{9.32}$$

Around $z = 0$ ($\mu b z \ll \hbar\gamma$) this expression can be expanded as a power series of $\mu b z/\hbar\gamma$.

Taking only the linear term into account yields with $\delta = \omega_L - \omega_0$:

$$F_z = -D \cdot z , \quad \text{with} \quad D = R_0 \mu \cdot b \frac{16k \cdot \delta}{\gamma^2 \left(1 + (2\delta/\gamma)^2\right)^2} . \tag{9.33}$$

We therefore obtain a restoring force that increases linearly increasing with z. The potential around the center of the MOT can be then described (because of $F_z = -\partial V/\partial z$) as the harmonic potential

$$V(z) = \frac{1}{2} D z^2 . \tag{9.34}$$

The atoms oscillate like harmonic oscillators around $z = 0$ and are spatially stabilized.

Note: There is a second force

$$F_\mu = -\boldsymbol{\mu} \cdot \operatorname{grad} \boldsymbol{B} ,$$

which acts on atoms with a magnetic moment in an inhomogeneous magnetic field.

Inserting the numbers for sodium atoms, it turns out that this force is negligibly small compared to the recoil force at laser powers in the milliwatt range. At very low temperatures, however, this force is essential to trap the atoms after the laser beams have been shut off (see Sect. 9.1.9)

In the discussion above we have neglected the velocity-dependent force in the optical molasses (Sect. 9.1.5).

The total force acting on an atom in the MOT

$$F_z = -Dz - av \,,$$

results in a damped oscillation around the center with an oscillation frequency

$$\Omega_0 = \sqrt{D/m} \,, \tag{9.35}$$

and a damping constant

$$\beta = a/m \,.$$

So far we have only considered the movement in the z-direction. The anti-Helmholtz coils produce a magnetic quadrupole field with three components. From Maxwell's equation $\operatorname{div} B = 0$ and the condition $\partial B_x/\partial x = \partial B_y/\partial y$, which follows from the rotational symmetry of the arrangement, we obtain the relations

$$\frac{\partial B_x}{\partial x} = \frac{\partial B_y}{\partial y} = -\frac{1}{2}\frac{\partial B_z}{\partial z} \,.$$

The restoring forces in the x- and y-directions are therefore half of the forces in z-directions. The trapped thermal cloud of atoms fills an ellipsoidal volume.

Instead of using counter-propagating laser beams with σ^+ and σ^- polarization, one can also cool the atoms if the two beams have the same polarization but slightly different frequencies $\omega^+ = \omega_0 + \Delta\omega$ and $\omega^- = \omega_0 - \Delta\omega$, which guarantees that the atoms moving out of the trap are pushed back. These frequencies can be produced as the two sidebands generated by acousto-optic modulation of the incident laser beam tuned to the center frequency ω_0 of the atomic transition.

Example 9.9.

With a magnetic field gradient of 0.04 T/m a sodium atom at $z = 0$ in a light trap with two counterpropagating σ^+-polarized laser beams L^+, L^- in the $\pm z$-direction with $I_+ = 0.8 I_{\text{sat}}$, $\omega_+ = \omega_0 - \gamma/2$ and $I_- = 0.15 I_{\text{sat}}$, $\omega_- = \omega_0 + \gamma/10$, the negative acceleration of a Na atom moving away from $z = 0$ reaches a value of $a = -3 \times 10^4\ \text{m/s}^2$ ($\hat{=} 3 \times 10^3 g$!), driving the atom back to $z = 0$.

Generally, the MOT is filled by slowing down atoms in an atomic beam (see Sect. 9.1.3). Spin-polarized cold atoms can also be produced by optical pumping in a normal vapor cell and trapped in a magneto-optic trap. This was demonstrated by Wieman and coworkers [9.54b], who captured and cooled 10^7 Cs atoms in a low-pressure vapor cell by six orthogonal intersecting laser beams. A weak magnetic field gradient regulates the light pressure in conjunction with the detuned laser frequency to produce a damped harmonic motion of the atoms around the potential minimum. This arrangement is far sim-